RESEARCH ARTICLE
SPACE PHYSICS: MAGNETOSPHERIC PHYSICS

Earth and Planetary Physics
1: 2-12, 2017
doi: 10.26464/epp2017002

Corotating drift-bounce resonance of plasmaspheric electron with poloidal ULF waves

Qiu-Gang Zong[1]*, YongFu Wang[1], Jie Ren[1], XuZhi Zhou[1], SuiYan Fu[1], Robert Rankin[2], and Hui Zhang[3]

[1]Institute of Space Physics and Applied Technology, Peking University, Beijing, China;
[2]Department of Physics, University of Alberta, Edmonton, Alberta, Canada;
[3]Physics Department and Geophysical Institute, University of Alaska Fairbanks, Fairbanks, USA

Abstract: The purpose of this paper is to understand how low energy plasmaspheric electrons respond to ULF waves excited by interplanetary shocks impinging on magnetosphere. It is found that both energy and pitch angle dispersed plasmaspheric electrons with energy of a few eV to tens of eV can be generated simultaneously by the interplanetary shock. The subsequent period of successive dispersion signatures is around 40 s and is consistent with the ULF wave period (third harmonic). By tracing back the energy and pitch angle dispersion signatures, the position of the electron injection region is found to be off-equator at around -32° in the southern hemisphere. This can be explained as the result of injected electrons being accelerated by higher harmonic ULF waves (e.g. third harmonic) which carry a larger amplitude electric field off-equator. The dispersion signatures are due to the flux modulations (or accelerations) of "local" plasmaspheric electrons rather than electrons from the ionosphere. With the observed wave-borne large electric field excited by the interplanetary shock impact, the kinetic energy can increase to a maximum of 23 percent in one bouncing cycle for plasmaspheric electrons satisfying the drift-bounce resonance condition by taking account of both the corotating drift and bounce motion of the local plasmaspheric electron.

Keywords: drift-bounce resonance; plasmaspheric electron; poloidal mode; ULF wave

Citation: Zong, Q. G., Y. F. Wang, J. Ren, X. Z. Zhou, S. Y. Fu, R. Rankin, and H. Zhang (2017). Corotating drift-bounce resonance of plasmaspheric electron with poloidal ULF waves. *Earth Planet. Phys.*, *1*, 2-12. http://doi.org/10.26464/epp2017002

1. Introduction

Sudden plasma density and/or velocity changes in the solar wind, e.g., dynamic pressure pulses or interplanetary shocks will lead to a step-like enhancement of the solar wind dynamic pressure. When such a structure impinges on the Earth's magnetosphere, the magnetosphere will be suddenly compressed, causing fast magnetosonic mode ULF waves that propagate into the magnetosphere (Wilken et al., 1982; Kepko and Spence, 2003; Hudson et al., 2004; Claudepierre et al., 2009). These fast magnetosonic waves will couple to and thus excite the local standing Alfvén waves through the field line resonance (FLR) process at the dayside magnetosphere around magnetic local noon (Southwood, 1974; Chen L and Hasegawa, 1974; Zhang XY et al., 2010).

It is known that the impingement of interplanetary shocks on Earth's magnetosphere can trigger/generate various type of waves including harmonic radiations with a few hundreds Hz (Hayashi et al., 1978), fast magnetosonic waves (Wilken et al., 1982; Kepko and Spence, 2003; Hudson et al., 2004; Claudepierre et al., 2009), whistler waves (Park, 1975), EMIC waves (Anderson and Hamilton, 1993), chorus waves (Fu HS et al., 2012), toroidal mode ULF standing waves (Cahill et al., 1990) and both poloidal and toroidal ULF waves (Zong Q-G et al., 2009; Zhang XY et al., 2010) in the geospace. These generated waves can further interact with particles and lead to energetic electron acceleration (Li XL et al., 1993; Zong Q-G et al., 2009; Tan LC et al., 2011) in the radiation belt, and ion acceleration in the ring current region (Zong Q-G et al., 2012).

Nevertheless, the shock-related energetic particle acceleration mechanism is still not fully understood (Baker et al., 2004; Friedel et al., 2002), although very energetic particle acceleration (ions and electrons with energies up to 15 MeV) in the inner magnetosphere due to the impact of an extreme powerful interplanetary shock on 24 March 1991 has been reported (Blake et al., 1992; Vampola and Korth, 1992; Wygant et al., 1994; Looper et al., 1995). In fact, recently, in situ observations of the resonance between energetic electrons and ULF waves (Zong Q-G et al., 2007; Tan LC et al., 2004, 2011) have been reported. Because of the comparable periods between the drift motion of the energetic particles and the ULF oscillations, the drift-bounce resonance interaction (e.g., Southwood and Kivelson, 1981; Hudson et al., 2008; Zong Q-G et al., 2007; Zong Q-G et al., 2009) could be excited to adiabatically accelerate the magnetospheric particles and significantly enhance the radial diffusion coefficient (e.g., Loto'aniu et al., 2006).

An excellent example of the interaction between ULF waves induced by an interplanetary shock and resulting energetic elec-

Correspondence to: Q.-G. Zong, qgzong@pku.edu.cn
Received 27 FEB 2017; Accepted 04 APR 2017.
Accepted article online 11 AUG 2017.

trons in the magnetosphere has been investigated by Zong Q-G et al., (2009). Zong Q-G et al. (2009) studied the acceleration process of energetic electrons with energy higher than 30 keV in the outer radiation belt November 7, 2004 event. In this case, the acceleration of energetic electrons by poloidal mode ULF waves starts immediately after the interplanetary shock arrival and lasts for at least a few hours. Zong Q-G et al. (2012) also investigated the response of plasma and energetic ions to the interplanetary shock impact, and the contribution to the ion acceleration of both poloidal and toroidal electric fields carried by ULF waves. Furthermore, it is suggested that drift resonance with poloidal ULF waves (Zong Q-G et al., 2009) or compressional poloidal mode ULF waves (Tan LC et al., 2011) induced by interplanetary shock impact will lead to fast electron acceleration and formation of the new radiation belt (Zong Q-G et al., 2011).

Recently, on the other hand, Zong Q-G et al. have reported that low-energy ring current O^+ ions (several to tens of keV) may be accelerated or decelerated by ULF standing waves via drift-bounce resonance during storm times (Yang B et al., 2010, 2011a, b; Zong Q-G et al., 2011, 2012). It has also been suggested that the ring current ions (especially H^+) having a free energy source can produce ULF waves through drift-bounce resonance in the inner magnetosphere (e.g., Hughes et al., 1978; Glassmeier et al., 1999; Wright et al., 2001; Ozeke and Mann, 2008).

Plasma ion accelerations in the field-align direction due to the interplanetary shocks impact have been addressed by (Olson and Lee, 1983; Yue C et al., 2016). It is shown that the acceleration in the field-align direction can be estimated with the proportional to the power of local magnetic field strength due to the magnetic field compressions caused by the interplanetary shock impinge on the magnetosphere (Yue C et al., 2016). Also, it is noticed that plasma electron can be heated by the interplanetary shock impact, however, this process can not be explained by the $\boldsymbol{E}\times\boldsymbol{B}$ drift and the above mentioned the adiabatic acceleration (Yue C et al., 2016).

A schematic overview of the wave power for various waves (ULF, VLF) and the drift, bounce and gyro frequency of electrons in the inner magnetosphere are shown in Figure 1. Usually lower frequency waves contain more wave power and the wave power scales roughly inversely with the wave frequency (Lanzerotti and Southwood, 1979). The overlap area between the wave frequency and the drift, bounce and gyro frequency of electrons indicates that wave-electron resonance may occur. Figure 1 is just a schematic overview, the details of wave-particle resonant condition should consider the wave frequency and wave vector, wave harmonic number, the location and the particles' pitch angle distribution etc.

In this paper, we shall investigate how plasmaspheric electrons (<100 eV) respond to the interplanetary shock impact and the interactions between plasmaspheric electrons (<100 eV) and poloidal ULF waves in the inner magnetosphere. The observations presented show that poloidal ULF waves excited by interplanetary shock impact can accelerate and heat the plasmaspheric electrons.

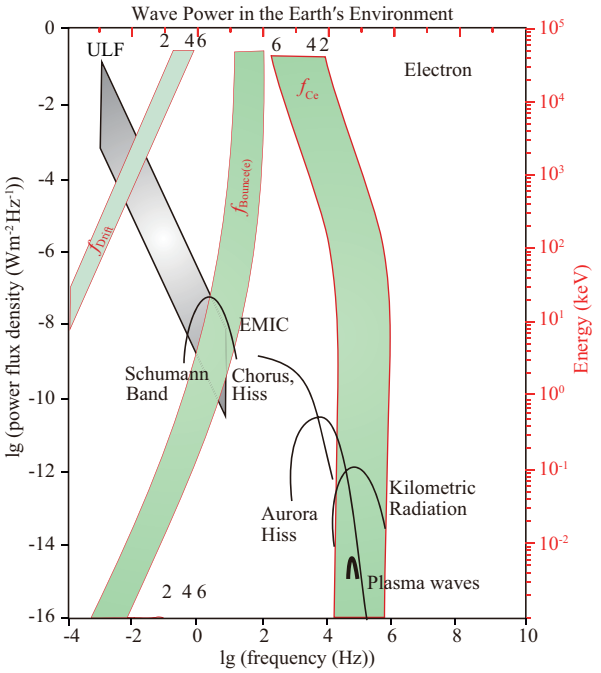

Figure 1. Overview of the possible ULF or VLF wave interactions with energetic electrons in Earth's inner magnetosphere. The figure shows the power flux density of various kinds of waves (left *Y*-axis) with different frequencies, the gyration, bounce, and drift frequencies of energetic electrons with different energies in different *L*-shells (right *Y*-axis). The frequency range of ULF waves overlaps the bounce and drift frequency of electrons, therefore both the bounce and drift resonance may occur between ULF waves and energetic electrons (Zong Q-G et al., 2008).

2. Plasmaspheric Electrons Interacting with ULF Waves Generated by Interplanetary Shock Impact

2.1 Electron Behavior

To inspect how plasmaspheric electrons respond to an interplanetary shock, we summarize Cluster C3 observations (Escoubet et al., 1997) from various instruments in Figure 2. The energetic electron measurements were obtained by the RAPID instrument (Wilken et al., 2001), the low energy electron measurements were taken from PEACE instrument (Johnstone et al., 1997), the magnetic field measurements were from the fluxgate magnetometer (FGM) (Balogh et al., 1997), the electric field data from the EFW instrument (Gustafsson et al., 2001) and the plasma data from the Cluster Ion Spectrometry (CIS) Experiment (Rème et al., 1997) onboard CLUSTER.

Low energy and energetic electron spectrograms in the energy range from 3 eV to 500 keV obtained by the Cluster PEACE and RAPID instruments are plotted in the top two panels of Figure 2. Observed magnetic fields and electric fields are plotted in the third and fourth panels of of Figure 2. In the fifth and sixth panels are the toroidal (B_a, E_r) and poloidal (B_r, E_a) wave magnetic and electric fields which are obtained from the magnetic and electric fields projected onto a local mean-field-aligned (MFA) coordinate system. In the MFA coordinate system, the parallel direction $\boldsymbol{p}$ is determined by 10-min sliding averaged magnetic field, the azi-

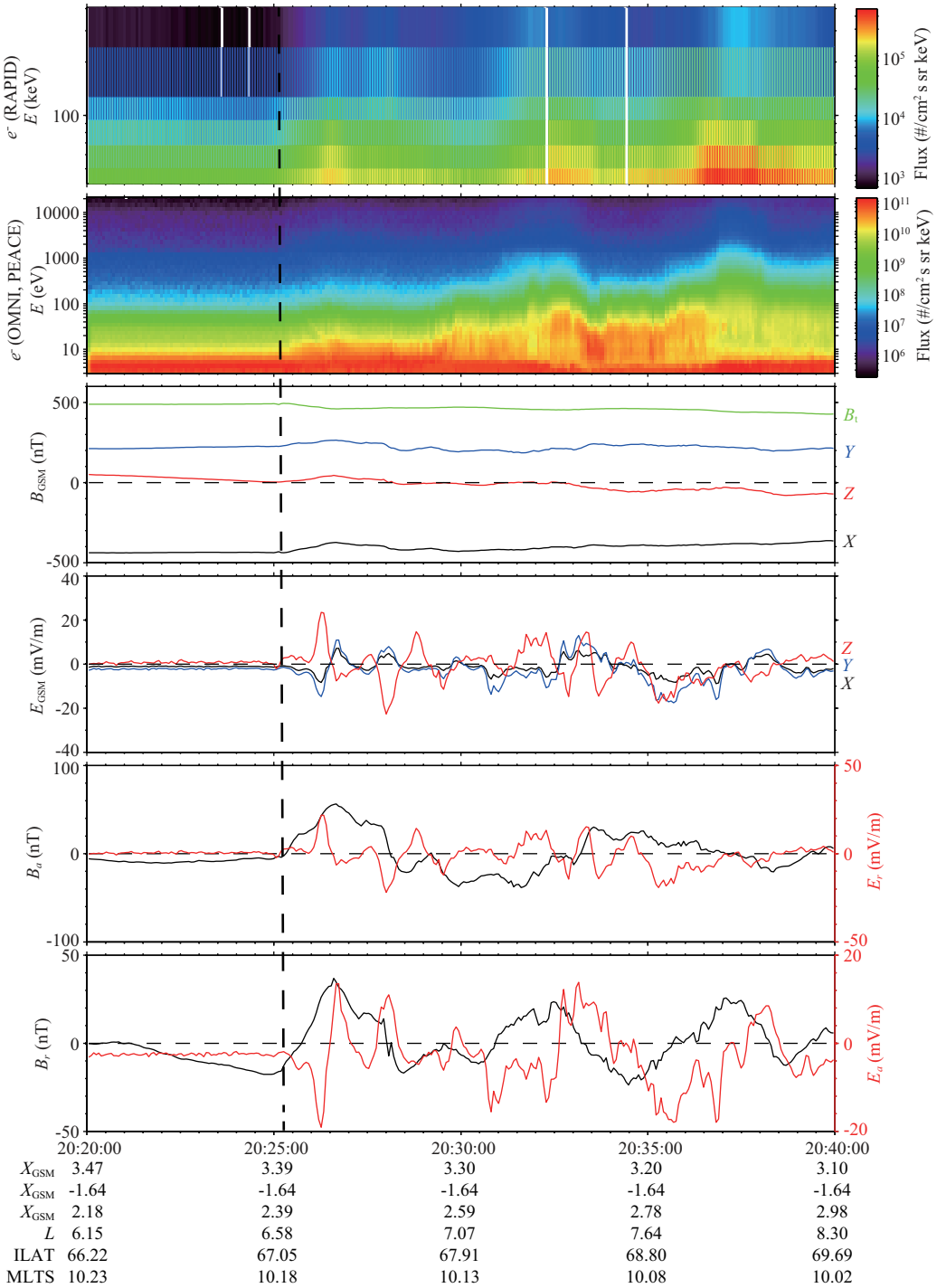

Figure 2. Electrons in the inner magnetosphere response to the interplanetary shock impact. From top to bottom: Panel 1 and 2 are the electron spectrogram with energy from 3 eV to 40 keV and 30 keV to 500 keV respectively; Panel 3 and 4 show observed magnetic field and electric components (*X*-black, *Y*-blue, and *Z*-red); Panel 5 and 6 show the toroidal (B_a, E_r) and poloidal (B_r, E_a) wave magnetic and electric fields. The equatorial radial distance in R_E (the L value) for C3 is given in the labels at the bottom. The vertical dashed line marks the arrival time of the interplanetary shock at 20:25:10UT.

muthal direction ***a*** is parallel to the cross product of the ***p*** and the spacecraft position vector, and the radial direction ***r*** completes the triad. As shown in Figure 2, Cluster satellites lied on the morning side (MLT~10.2) of the magnetosphere (L=6.6) at that time and observed ULF waves induced by the interplanetary shock impacting on the magnetosphere, the amplitude of the electric field is ~50 mV/m.

The interplanetary shock arrival time is marked by the vertical dashed line. As shown in Figure 2, the electrons (3 eV to 500 keV) were simultaneously accelerated or heated with the shock arrival, the rapid electron acceleration or heating could be directly correlated with the impact of the interplanetary shock on 25 Septem-

ber 2001.

As reported by Tan LC et al. (2011), during this event, magnetospheric ULF waves have been excited with a wave number ≈3 and consequently relativistic electrons (up to MeV electrons) are accelerated by those ULF waves with a time scale of a few hours. In this paper, we shall focus on how the excited ULF waves interact with plasmaspheric electrons (<100 eV).

In order to examine how plasmaspheric electrons (<100 eV) in the inner magnetosphere response to the interplanetary shock impact in detail, representative electron pitch angle distributions for fourteen energy channels ranging between 5 and 72.5 eV are given in Figure 3.

As we can see from Figure 3, one outstanding and surprising feature is electron pitch angle dispersion with the field-aligned (0°) electron observed first, and the anti-field-aligned (180°) electron observed last immediately after the interplanetary shock arrival. Such a pitch angle dispersion can be clearly seen for seven energy channels from 6 to 19.9 eV. Above 19.9 eV, one can see the electron pitch angle oscillate between (0°) and (180°), no clear pitch angle dispersion signature can be seen.

The multi dispersions are marked in black dashed lines for easy distinguishing. It should be noticed here that the occurring period of successive dispersion signatures is around 40 s and in consistence with the ULF wave period. Thus, these multi-dispersions may be the results of modulation by ULF wave oscillations.

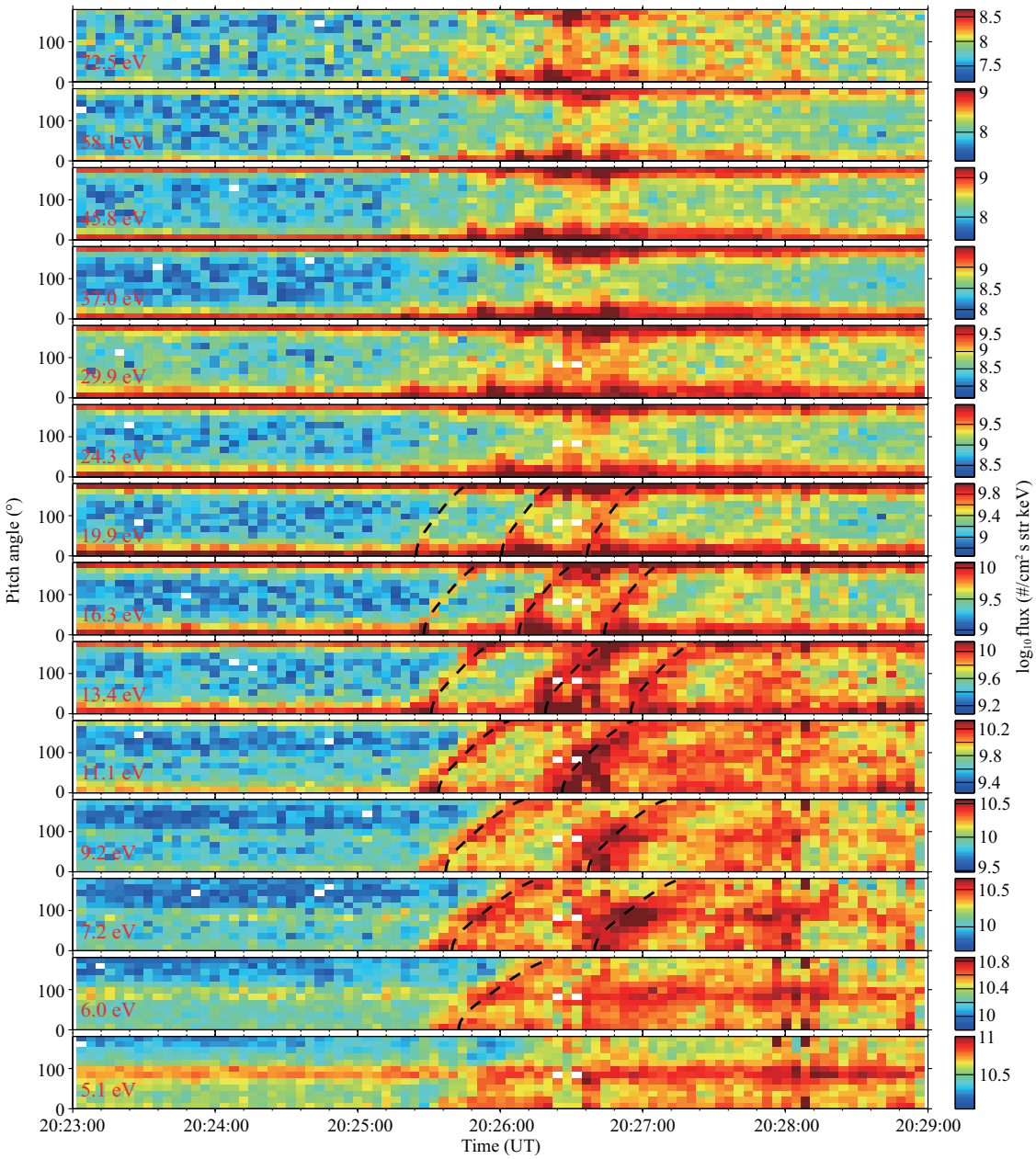

Figure 3. Pitch angle distributions of low energy electron in the inner magnetosphere response to the interplanetary shock impact. From top to bottom: representative electrons with pitch angle distributions for fourteen energy channels ranging between 5 and 72.5 eV.

The pitch angle dispersion phenomena is further confirmed by the energy dispersion shown in Figure 4. The multiple energy dispersions appear in the parallel (Figure 4a and anti-parallel (Figure 4c) direction almost simultaneously after the interplanetary shock arrival at 20:25:10 UT.

With both the pitch angle (Figure 3) and energy (Figure 4) dispersion signatures, the location of the electron injection (possibly acceleration location) can be estimated by using the method of the time of flight (Zong Q-G et al., 2001; Korth et al., 2004). Considering two electrons with different pitch angles at the same energy, the one with smaller pitch angle would precede the one with larger pitch angle. However, it should be noted that particle's speed along the field line will be changed when the amplitude of the magnetic field changes because of the conservation of the first adiabatic invariant (Zong Q-G et al., 2012).

The energy dispersions in the parallel direction appeared earlier than those in the anti-parallel direction, the first two dispersion signatures lead about 32.6 s and the third signature leads about 30.3 s. The electron with an energy of several eV travels from the equator to its mirroring point (or vice versa) in a quarter of its bounce period. Assuming that the electrons of different energy bounced from the same source region and reached the spacecraft, the reaching time delay can be calculated using the dipole field model (Roederer, 1970, e.g.). This is basically consistent with the observed lead time of dispersion (about 35 s). The occurring period of successive dispersion signatures is around 40 s and in consistence with the ULF wave period (third harmonic, see next section), indicating these dispersion signatures were due to the flux modulations (or accelerates) of "local" (plasmaspheric, rather than the electron from the Earth's ionosphere) electrons by ULF waves. Further analysis shows that electrons with energies of several eV satisfied the drift-bounce resonance condition in this case.

As labeled at the bottom of Figure 2, the Cluster spacecraft were located in the the northern hemisphere (~37.5° MLAT, ~10 MLT). Tracing back both the electron's pitch angle and energy disper-

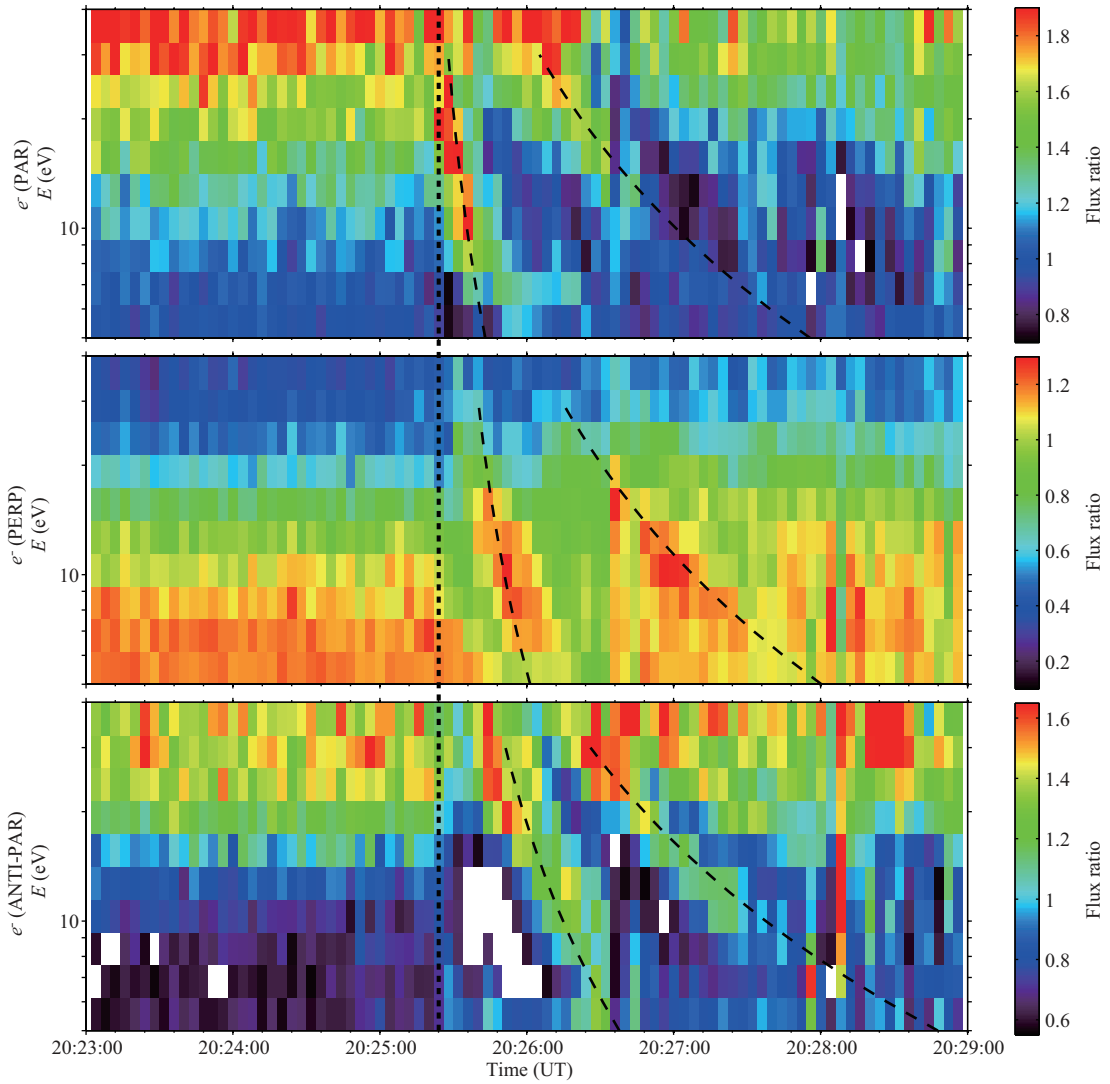

Figure 4. Electron energy dispersion. Top panel: electron spectrogram of flux ratio of parallel direction to omni-direction; middle panel: electron spectrogram of flux ratio of perpendicular direction to omni-direction; bottom panel: electron spectrogram of flux ratio of anti-parallel direction to omni-direction. The shock arrival time is marked by the vertical dashed line.

sion signatures, the location of the electron injection can be estimated at around -32° of the southern hemisphere, as can be seen in Table 1. Thus, the acceleration region of the observed plasma electron is located at southern hemisphere of the same *L*-shell.

Table 1. Electron Source Location

	Location(Lat.)	Injection Time (UT)	Interval (sec)
Pitch angle dispersion	-29°	20:25:05	46
Energy dispersion	-35.2°	20:25:11	42

Different with MeV electrons (Zong Q-G et al., 2009) and ring current ions (Zong Q-G et al., 2012) (for which the acceleration locations are found to be near the equator region), the location of these low energy electrons is estimated at around -32° off the southern hemisphere for both the pitch angle and energy dispersion signatures. The obtained injection time 20:25:08 UT (Table 1) is in agreement with the arrival time of the interplanetary shock.

2.2 The Variation of Electron Spectra

So as to examine the plasmaspheric electron flux variation, electron spectra (Figure 3 and Figure 4) obtained by PEACE instrument with 4 sec time resolution for two different time intervals-immediately after the shock arrival (20:25:30 UT, blue), and after the first dispersion signal (20:26:05 UT, red) are given in Figure 5.

As we can see from Figure 5, immediately after the interplanetary shock impact at 20:25:30 UT, the electron spectrum was still flat. However, after the first pitch angle and energy dispersion at 20:26:05 UT, there are well developed double-peak structures in the electron spectrum; one peak is between 5 eV and 6 eV, the other peak is between 15 eV and ~20 eV.

As discussed in (Zong Q-G et al., 2012), the energy variation of particles in the inner magnetosphere can be expressed as (Northrop, 1963)

$$\dot{W} = qE_{\perp}\cdot v_d + qE_{/\!/}v_{/\!/} + \mu\frac{\partial B_{/\!/}}{\partial t}, \qquad (1)$$

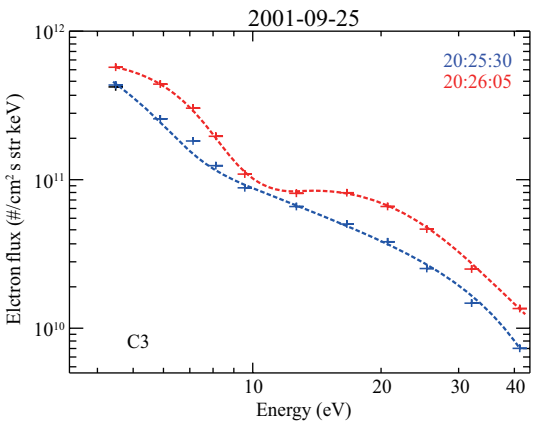

Figure 5. Plasmaspheric electron spectra observed by PEACE instruments on board Cluster C3, immediately after (2025 UT, blue), and after the shock arrival (2026 UT, red) for the 25 September 2001 event.

where $\dot{W}$ is the rate of energy change, $E_{\perp}$ is the perpendicular component of electric field, v_d is the gradient and curvature drift velocity, $v_{/\!/}$ and $E_{/\!/}$ are the parallel component of electric field and particle velocity, and $B_{/\!/}$ is the compressional component of the magnetic field.

This equation suggests that the particle energy variation in the inner magnetosphere can be divided into three parts: the first term on the right hand side represents the acceleration of the drifting particles caused by the perpendicular electric field, the second term is due to the effect of parallel electric field, and the third term is the contribution of the compressional component of the magnetic field. The parallel electric field is usually neglected since it can not be built up in a collisionless plasma environment. Thus, when an interplanetary shock impinges on the magnetosphere, the energetic electron (Zong Q-G et al., 2009) and plasma ions (Zong Q-G et al., 2012) can be accelerated by the ULF waves carried electric field.

When an interplanetary shock impinges on the magnetosphere, the magnetosphere will be compressed. Due to the size of the magnetosphere and the Alfvén speed, the interaction time scale is around ~1 min. Thus, it is a reasonable assumption that the first adiabatic invariant is conserved during an interplanetary shock impact (Wilken et al., 1986).

In order to consider the particle acceleration contributed by the compressional component of the magnetic field (the third term of Eq. (1)), the variation of the magnetic field due to the interplanetary shock compression should be considered. The energy change of particles can be estimated by using the third term in Eq. (1) assuming a conserved magnetic moment, the energy change of particles are energy dependent.

As we can see from Figure 2, after the shock compression, all magnetic field components (B_x, B_y, B_z) changed little, the amplitude of magnetic field (B_t) even turned to decrease. This leads the $<\partial B_{/\!/}/\partial t>$ term was rather small and can be ignored. Thus, the shock compression has a limited effect as reflected on electron spectra both in Figures 5 and Figure 2. This implies that the electric field carried by ULF waves have a major contribution to the plasmaspheric electron heating/acceleration after the interplanetary shock arrival.

3. Discussion and Interpretation

In this paper, we have studied the interaction between low energy electrons (<100 eV) and poloidal ULF waves in the inner magnetosphere or plasmaspheric region and investigated how plasmaspheric electron (<100 eV) in the inner magnetosphere respond to the interplanetary shock impact. The observations presented show that poloidal ULF waves excited by interplanetary shock impact can heat and accelerate low energy electron (<100 eV) in the radiation belt region.

For the particle acceleration in the parallel direction due to the impact of IP shocks (Olson and Lee, 1983; *Yue C et al.*, 2016), performed a study to estimate the magnetic field compressions associated with sudden impulses and have shown that the plasma average energy in the parallel direction is proportional to the power of local magnetic field strength if the first and second adiabatic invariants are conserved (Yue C et al., 2016).

Besides the *E*×*B* drift and adiabatic acceleration, what are the other mechanisms responsible to the electron acceleration? Addressing the above issues would contribute to a better understanding of the responses of the inner magnetosphere to IP shock impacts.

3.1 The Correlation Between the Electron and ULF Waves

To quantify the correlation between observed ULF waves generated by the interplanetary shock impact and plasmaspheric electrons, the wavelet coherence (Grinsted et al., 2004) between the electric field components and the electron flux (the top three panels for poloidal mode, the bottom three panels for toroidal mode) are calculated and shown in Figure 6. The poloidal and toroidal electric field and magnetic fields are obtained by decomposing the Cluster magnetic field and electric field into a MFA coordinate

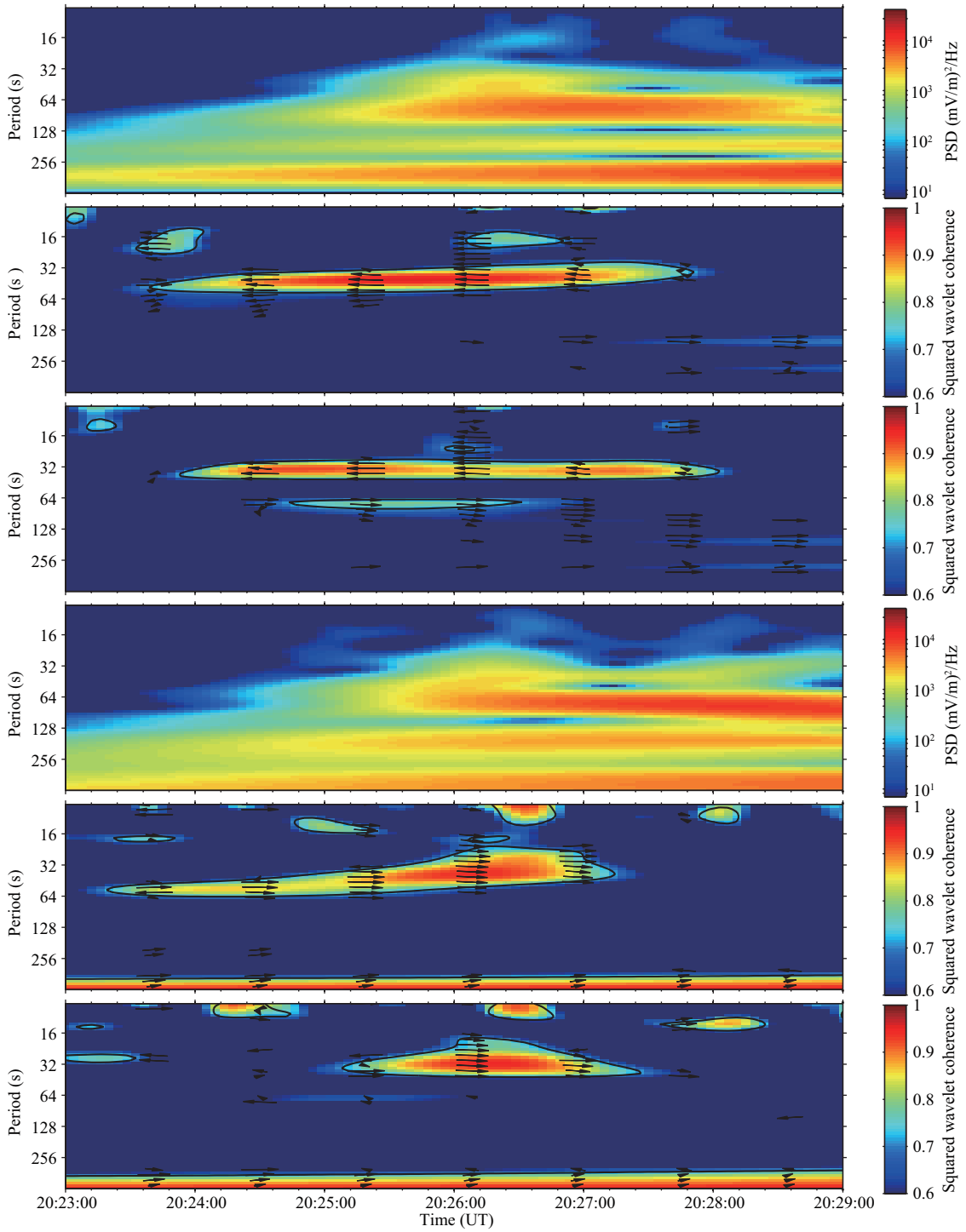

Figure 6. Continuous wavelet power spectrum of both ULF poloidal and toroidal electric field and the squared wavelet coherence between the poloidal mode and toroidal mode electric field and parallel (pitch angle <45°) electron flux at 16.335 eV and perpendicular (pitch angle >45°) electron flux.

system (Takahashi et al., 1990).

As shown in Figure 6, the top panel is the continuous wavelet power spectrum of the azimuthal electric field (ULF poloidal mode), Panels 2 and 3 are the squared wavelet coherence between the azimuthal electric field and parallel (pitch angle <45°) electron flux at 16.335 eV and perpendicular (pitch angle >45°) electron flux. Panel 4 is the wavelet power spectrum of the radial electric field (ULF toroidal mode), Panels 5 and 6 are the squared wavelet coherence between the radial electric field and parallel (pitch angle <45°) electron flux at 16.335 eV and perpendicular (pitch angle >45°) electron flux.

Although the poloidal (Panel 1) and toroidal (Panel 4) waves have similar power intensity, the coherences are quite different. Very high coherence (above 0.9) appears in the poloidal mode more significant than the toroidal mode after the shock arrival at 20:25:15 UT. It should be noted here that the ULF wave band which highly correlated with parallel (pitch angle <45°) electron flux is among 32 to 64 s, whereas the ULF wave band which is highly correlated with the perpendicular (pitch angle >45°) electron flux is around 32 s.

The duration of high coherence for the poloidal mode is longer than that for the toroidal mode. In the wavelet coherence analysis of Figure 6, the black arrows pointing to the left and right represent that the phase angles are 180° and 0°, respectively. The phase angles between the poloidal mode electric field and both the parallel (pitch angle <45°) electron flux and the perpendicular electron (pitch angle >45°) flux are nearly 0°, indicating the positive correlation between the poloidal mode ULF waves and the electron flux. However, on the other hand, the phase angles between the toroidal mode electric field and both the parallel (pitch angle <45°) electron flux and the perpendicular (pitch angle >45°) electron flux are nearly 180°, indicating the anti-correlation between the toroidal mode ULF waves and the electron flux.

These results indicate the strong correlation between both the poloidal (E_a) and toroidal (E_r) mode ULF wave electric field and the plasmaspheric electrons. The close correlation between the ULF wave electric field E_r and E_a oscillations and the electron flux suggests that the shock-induced ULF waves had strong heating/acceleration effects on the plasmaspheric electrons. The correlation between the observed ULF waves and electrons above 19.9 eV are much weaker comparing to that of electrons at 16.335 eV (not shown here).

3.2 Electron-ULF Wave Resonance

The strong correlation between both ULF waves and plasmaspheric electron can be ex-plained by the framework proposed by Southwood and Kivelson (Southwood and Kivelson, 1981; Southwood and Hughes, 1982). In their work, particles experience the electric field carried by ULF waves during their drift-bounce motions in the inner magnetosphere and these particles' energy can be accordingly changed depending on their paths.

The condition of the resonance between the particle and the ULF waves-the bounce drift resonance can be determined by

$$\Omega - m \cdot \omega_d = N \cdot \omega_b, \tag{2}$$

where N is an integer (normally ±1, ±2 or 0), m represents the azimuthal wave number of the ULF wave, and Ω, ω_d and ω_b are the wave frequency, the drift and bounce frequencies of the particle, respectively. For a particle with given energy in the inner magnetosphere, the drift and bounce frequencies of the particle (ω_d, ω_b) can be computed at a given L-shell, thus, the resonance energy can be determined if the wave frequency (Ω) and the wave number (m) are known.

For a plasmaspheric electron with a energy of a few eV in the inner magnetosphere, the drift frequency of the electron is much less than the bounce frequency: $\omega_d \ll \omega_b$), thus, the bounce-drift resonance between the plasmaspheric electron and the ULF waves becomes the bounce resonance:

$$\Omega = N \cdot \omega_b. \tag{3}$$

It is worth pointing out that the resonant condition of the bounce resonance is independent of wave number, which implies that plasmaspheric electron could resonant with either poloidal mode or toroidal mode ULF or both. As shown in Figure 6, the flux variations of plasmaspheric electron are indeed correlated with both poloidal mode and toroidal mode ULF waves. The high correlation is mainly in the period range from 30 s to 60 s. Assuming that L=7, particle energy is from 6 eV to 20 eV, equatorial pitch angle is 30°, the bounce period is from 69 s to 137 s. The bounce period of the cold electrons is almost two times of the wave period in high correlation, which indicates that these cold electrons satisfy the drift-bounce resonant condition of N=2. The toroidal mode has time varying radial electric field and azimuthal magnetic field, and the poloidal mode has azimuthal electric field and radial magnetic field perturbations (Zong Q-G et al., 2009, 2012; Zhang XY et al., 2009), although large-scale compressional waves may also contribute to the azimuthal electric field oscillations to some extent (Hudson et al., 1997). When the geomagnetic field is in the noon-midnight asymmetry under the solar wind impact, the drift velocity of the cold electrons will have a component in the radial direction, but the electron energy will be changed after a drifting period (about 1 day). However, the cold electrons are rapidly accelerated/heated after the drift-bounce resonance with ULF waves in Figure 7, which suggests that the acceleration/heat of the cold electrons are from the interaction with poloidal waves but not toroidal waves.

Figure 7 illustrated a bounce resonant plasmaspheric electron motion in the rest frame of (a) fundamental, (b) second, and (c) third harmonic standing mode wave, the dashed lines represent the electron trajectory. Plasmaspheric electron are moving in the trajectory represent by dashed lines in the wave rest frame, which is the same direction as the electric field E_a carried by the poloidal ULF waves. Therefore, the negative (positive) E_a would accelerate (decelerate) plasmaspheric electron when it is resonant with ULF waves, which agrees with our observations (Figure 3 and Figure 4) very well.

It should be noted that for most plasmaspheric electrons, the acceleration and deceleration processes would cancel out the energy gain within one wave period. As we can see from Figure 7, electron resonant with fundamental mode would cancel out the

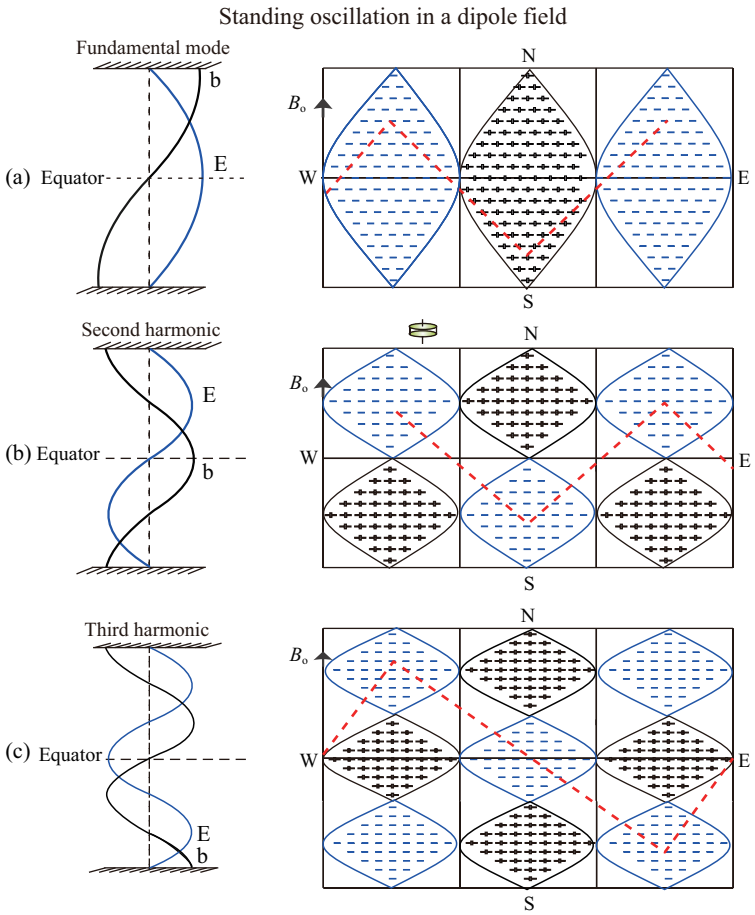

Figure 7. Illustration of the bounce resonance (after Southwood and Kivelson (1982)) for (a) fundamental, (b) second, and (c) third harmonic standing mode. The dashed lines represent the electron motion in the rest frame of the wave.

energy gain within one wave period, only those plasmaspheric electrons resonant second or third harmonic ULF waves can gain energy very efficiently.

The energy change of resonant particles with ULF waves can be expressed as

$$\frac{\mathrm{d}w}{\mathrm{d}t} = qE_aV_d,$$

where $\frac{\mathrm{d}w}{\mathrm{d}t}$, E_a, and V_d are the rate of the particle energy, the poloidal wave azimuthal electric field, and the particle velocity in the wave frame respectively.

More and more observations have revealed the importance of ULF waves in the dynamics of radiation belt electrons and ring current ions. This study reports that cold plasmaspheric electrons also could be accelerated/heated through the drift-bounce resonance with ULF waves, which provides a new acceleration mechanism for the low energy plasmaspheric electrons and may also explain the thinning of the plasmasphere. In another ongoing work, we found that low-energy (15 eV-200 eV) plasmaspheric electron fluxes could be enhanced up to several times by ULF waves at the plasmaspheric boundary layer using Van Allen Probes data, and implied that colder electrons (~eV), out of the measurements of Van Allen Probes, also can be affected by ULF waves. This new mechanism provides a new way to understand the plasmaspheric electron acceleration and heating.

4. Conclusion

The objective of this paper is to understand how plasmaspheric electrons response to the ULF waves excited by the impinge on magnetosphere of interplanetary shocks. Main results obtained in this paper can be summarized as fellows:

(1) Both plasmaspheric electron energy and pitch dispersion signatures generated by the interplanetary shock impinge on the magnetosphere are observed.

(2) Tracing back signatures from both energy and pitch dispersion, the position of the electron injection region is found to be off-equator-at around -32° of the southern hemisphere. This can be explained as that these injected electrons are accelerated by higher harmonic ULF waves (e.g. third harmonic) which having larger amplitude electric field off-equator. This is different with MeV electrons (Zong Q-G et al., 2009) and ring current ions (Zong Q-G et al., 2012) (which acceleration locations are found to be around the equator region).

(3) The occurring period of successive dispersion signatures is around 40 s and in consistence with the ULF wave period (third harmonic), indicating these dispersion signatures were due to the

flux modulations (or accelerations) of "local" (plasmaspheric, rather than the electron from the Earth's ionosphere) electrons by ULF waves.

(4) The duration of high coherence for the poloidal mode is longer than that for the toroidal mode. The phase angles between the poloidal mode electric field and both the parallel (pitch angle <45°) electron flux and the perpendicular (pitch angle >45°) electron flux are nearly 0°, indicating the positive correlation between the poloidal mode ULF waves and the electron flux. On the other hand, the phase angles between the toroidal mode electric field and both the parallel (pitch angle <45°) electron flux and the perpendicular (pitch angle >45°) electron flux are nearly 180°, indicating the anti-correlation between the toroidal mode ULF waves and the electron flux. The close correlation between the ULF wave electric field E_r and E_a oscillations and the electron flux suggests that the shock-induced ULF waves had strong heating/acceleration modulations on the plasmaspheric electrons.

In summary, plasmaspheric electron in the inner magnetosphere can be accelerated by ULF waves excited by an interplanetary shock impinging on Earth's magnetosphere. This mechanism requires that plasmaspheric electron satisfies the bounce resonance condition with poloidal mode ULF waves. Both observations and calculations show that plasmaspheric electron (~10 eV) can be accelerated very efficiently mainly by poloidal mode ULF waves.

Acknowledgments

This work was supported by National Natural Science Foundation of China National Natural Science Foundation of China (41421003 and 41627805). We acknowledge the instrument team of Cluster CIS, FGM, PEACE and STAFF for providing data.

References

Anderson, B. J., and Hamilton, D. C. (1993). Electromagnetic ion cyclotron waves stimulated by modest magnetospheric compressions. *J. Geophys. Res.*, *98*(A7), 11369-11382. https://doi.org/10.1029/93JA00605

Baker, D. N., Kanekal, S. G., Li, X., Monk, S. P., Goldstein, J., and Burch, J. L. (2004). An extreme distortion of the Van Allen belt arising from the 'Hallowe'en' solar storm in 2003. *Nature*, *432*, 878-881. https://doi.org/10.1038/nature03116

Balogh, A., Dunlop, M. W., Cowley, S. W. H., Southwood, D. J., Thomlinson, J. G., Glassmeier, K. H., Musmann, G., Lühr, H., Buchert, S., Acuña, M. H., Fairfield, D. H., Slavin, J. A., Riedler, W., Schwingenschuh, K., and Kivelson, M. G. (1997). The cluster magnetic field investigation. *Space Sci. Rev.*, *79*, 65-91. https://doi.org/10.1023/A:1004970907748

Blake, J. B., Kolasinski, W. A., Fillius, R. W., and Mullen, E. G. (1992). Injection of electrons and protons with energies of tens of MeV into l<3 on 24 March 1991. *Geophys. Res. Lett.*, *19*, 821-824. https://doi.org/10.1029/92GL00624

Cahill, L. Jr, J., Lin, N. G., Waite, J. H., Engebretson, M. J., and Sugiura, M. (1990). Toroidal standing waves excited by a storm sudden commencement: DE 1 observations. *J. Geophys. Res.*, *95*, 7857-7867. https://doi.org/10.1029/JA095iA06p07857

Chen, L., and A. Hasegawa (1974). A theory of long-period magnetic pulsations: 1. Steady state excitation of field line resonance. *J. Geophys. Res.*, *79*, 1024. https://doi.org/10.1029/JA079i007p01024

Claudepierre, S. G., Wiltberger, M., Elkington, S. R., Lotko, W., and Hudson, M. K. (2009). Magnetospheric cavity modes driven by solar wind dynamic pressure fluctuations. *Geophys. Res. Lett.*, *36*, L13101. https://doi.org/10.1029/2009GL039045

Escoubet, C. P., Russell, C. T., and Schmidt, R., (1997), *The Cluster and Phoenix Missions*, Kluwer Academic, Dordrecht, Netherlands..

Friedel, R. H. W., Reevesa, G. D., and Obara, T. (2002). Relativistic electron dynamics in the inner magnetosphere-a review. *J. Atmos. Solar-Terr. Phys.*, *64*, 265-282. https://doi.org/10.1016/S1364-6826(01)00088-8

Fu, H. S., Cao, J. B., Zong, Q.-G., Lu, H. Y., Huang, S. Y., Wei, X. H., and Ma, Y. D. (2012). The role of electrons during chorus intensification: Energy source and energy loss. *J. Atmos. Solar-Terr. Phys.*, *80*, 37-47. https://doi.org/10.1016/j.jastp.2012.03.004

Glassmeier, K.-H., Buchert, S., Motschmann, U., Korth, A., and Pedersen, A. (1999). Concerning the generation of geomagnetic giant pulsations by drift-bounce resonance ring current instabilities. *Ann. Geophys.*, *17*, 338-350. https://doi.org/10.1007/s00585-999-0338-4

Grinsted, A., Moore, J. C., and Jevrejeva, S. (2004). Application of the cross wavelet transform and wavelet coherence to geophysical time series. *Nonlin. Processes Geophys.*, *11*, 561-566. https://doi.org/10.5194/npg-11-561-2004

Gustafsson, G., André, M., Carozzi, T., Eriksson, A. I., Fälthammar, C.-G., Grard, R., Holmgren, G., Holtet, J. A., Ivchenko, N., Karlsson, T., Khotyaintsev, Y., Klimov, S., Laakso, H., Lindqvist, P.-A., Lybekk, B., Marklund, G., Mozer, F., Mursula, K., Pedersen, A., Popielawska, B., Savin, S., Stasiewicz, K., Tanskanen, P., Vaivads, A., and Wahlund, J.-E. (2001). First results of electric field and density observations by CLUSTER EFW based on initial months of operation. *Ann. Geophys.*, *19*, 1219-1240. https://doi.org/10.5194/angeo-19-1219-2001

Hayashi, K., Oguti, T., Watanbe, T., Tsuruda, K., Kokubun, S., and Horita R. E. (1978). Power harmonic radiation enhancement during the sudden commencement of a magnetic storm. *Nature*, *275*, 627-629. https://doi.org/10.1038/275627a0

Hudson, M. K., Elkington, S. R., Lyon, J. G., Marchenko V. A., Roth, I., Temerin M., Blake, J. B., Gussenhoven, M. S., and Wygant J. R. (1997). Simulations of radiation belt formation during storm sudden commencements. *J. Geophys. Res.*, *102*(A7), 14087-14102. https://doi.org/10.1029/97JA03995

Hudson, M. K., Denton, R. E., Lessard, M. R., Miftakhova, E. G., and Anderson, R. R. (2004). A study of Pc-5 ULF oscillations. *Ann. Geophys.*, *22*, 289-302. https://doi.org/10.5194/angeo-22-289-2004

Hudson, M. K., Kress, B. T., Mueller, H. R., Zastrow J. A., and Bernard Blake, J. (2008). Relationship of the Van Allen radiation belts to solar wind drivers. *J. Atmos. Solar-Terr. Phys.*, *70*, 708-729. https://doi.org/10.1016/j.jastp.2007.11.003

Hughes, W. J., McPherron, R. L., and Barfield, J. N. (1978). Geomagnetic pulsations observed simultaneously on three geostationary satellites. *J. Geophys. Res.*, *83*(A3), 1109-1116. https://doi.org/10.1029/JA083iA03p01109

Johnstone, A. D., Alsop, C., Burge, S., P. Carter, J., Coates, A. J., Coker, A. J., Fazakerley, A. N., Grande, M., Gowen, R. A., Gurgiolo, C., Hancock, B. K., Narheim, B., Preece, A., Sheather, P. H., Winningham, J. D., and Woodliffe, R. D. (1997). Peace: A plasma electron and current experiment. *Space Sci. Rev.*, *79*, 351-398. https://doi.org/10.1023/A:1004938001388

Kepko, L., and Spence, H. E. (2003). Observations of discrete, global magnetospheric oscillations directly driven by solar wind density variations. *J. Geophys. Res.*, *108*(A6), 1257. https://doi.org/10.1029/2002JA009676

Korth, A., Fränz, M., Zong, Q.-G., Fritz, T. A., Sauvaud, J.-A., Rème, Dandouras, H., Friedel, I., R., Mouikis, C. G., Kistler, L. M., Möbius, E., Marcucci, M. F., Wilber, M., Parks, G., Keiling, A., Lundin, R., and Daly, P. W. (2004). Ion injections at Auroral latitude during the March 31, 2001 magnetic storm observed by cluster. *Geophys. Res. Lett.*, *31*, L20806. https://doi.org/10.1029/2004GL020356

Lanzerotti, L. J., and Southwood, D. J. (1979), Hydromagnetic waves, In: Waite J. H. Jr, J. L. Burch, and R. L. Moore, eds., *Solar System Plasma Physics*, North-Holland Publishing Co., Amsterdam, 109-135..

Li, X. L., Roth, I., Temerin, M., Wygant, J. R., Hudson, M. K., and Blake, J. B. (1993). Simulation of the prompt energization and transport of radiation belt particles during the March 24, 1991 SSC. *Geophys. Res. Lett.*, *20*, 2423-2426. https://doi.org/10.1029/93GL02701

Looper, M. D., Blake, J. B., Mewaldt, R. A., Cummings J. R., and Baker, D. N. (1995).

Observations of the remnants of the ultrarelativistic electrons injected by the strong SSC of 24 March 1991. *Geophys. Res. Lett.*, *22*, 2079-2082. https://doi.org/10.1029/94GL01586

Loto'aniu, T. M., Mann, I. R., Ozeke, L. G., Chan, A. A., Dent, Z. C., and Milling, D. K. (2006). Radial diffusion of relativistic electrons into the radiation belt slot region during the 2003 Halloween geomagnetic storms. *J. Geophys. Res.*, *111*(A4), A04218. https://doi.org/10.1029/2005JA011355

Northrop, T. G (1963). Adiabatic charged-particle motion. *Rev. Geophys. Space Phys.*, *1*, 283-304. https://doi.org/10.1029/RG001i003p00283

Olson, J. V., and L. C. Lee (1983). Pc1 wave generation by sudden impulses. *Space Sci.*, *31*, 295C302. https://doi.org/10.1016/0032-0633(83)90079-X

Ozeke, L. G., and Mann, I. R. (2008). Energization of radiation belt electrons by ring current ion driven ULF waves. *J. Geophys. Res.*, *113*(A2), A02201. https://doi.org/10.1029/2007JA012468

Park, C. G (1975). Whistler observations during a magnetospheric sudden impulse. *J. Geophys. Res.*, *80*, 4738-4740. https://doi.org/10.1029/JA080i034p04738

Rème, H., Bosqued, J. M., Sauvaud, J. A., Cros, A., Dandouras J., Aoustin C., Bouyssou, J., Camus, T., Cuvilo J., Martz C., Médale, J. L., Perrier, H., Romefort, D., Rouzaud, J., D'Uston, C., Möbius, E., Crocker, K., Granoff, M., Kistler, L. M., Popecki, M., Hovestadt, D., Klecker B., Paschmann, G., Scholer, M., Carlson, C. W., Curtis, D. W., Lin, R. P., Mcfadden, J. P., Formisano, V., Amata, E., Bavassano-Cattaneo, M. B., Baldetti, P., Belluci, G., Bruno, R., Chionchio, G., Di Lellis, A., Shelley, E. G., Ghielmetti, A. G., Lennartsson, W., Korth, A., Rosenbauer, H., Lundin, R., Olsen, S., Parks, G. K., McCarthy, M., and Balsiger, H. (1997). The cluster ion spectrometry (CIS) experiment. *Space Sci. Rev.*, *79*, 303-350. https://doi.org/10.1023/A:1004929816409

Roederer, J. G. (1970), *Dynamics of Geomagnetically Trapped radiation*, Springer-Verlag, New York..

Southwood, D. J. (1974). Some features of field line resonances in the magnetosphere. *Planet. Space Sci.*, *22*, 483-491. https://doi.org/10.1016/0032-0633(74)90078-6

Southwood, D. J., and Kivelson, M. G. (1981). Charged particle behavior in low-frequency geo-magnetic pulsations. 1. Transverse waves. *J. Geophys. Res.*, *86*(A7), 5643-5655. https://doi.org/10.1029/JA086iA07p05643

Southwood, D. J., and Hughes, W. J. (1982). Theory of hydromagnetic waves in the magnetosphere. *Space Sci. Rev.*, *35*, 301-366. https://doi.org/10.1007/BF00169231

Takahashi, K., McEntire, R. W., Lui, A. T. Y., and Potemra, T. A. (1990). Ion flux oscillations associated with a radially polarized transverse Pc 5 magnetic pulsation. *J. Geophys. Res.*, *95*(A4), 3717-3731. https://doi.org/10.1029/JA095iA04p03717

Tan, L. C., Fung, S. F., and Shao, X. (2004). Observation of magnetospheric relativistic electrons accelerated by Pc-5 ULF waves. *Geophys. Res. Lett.*, *31*, L14802. https://doi.org/10.1029/2004GL019459

Tan, L. C., Shao, X., Sharma, A. S., and Fung, S. F. (2011). Relativistic electron acceleration by compressional-mode ULF waves: Evidence from correlated Cluster, Los Alamos National Laboratory spacecraft, and ground-based magnetometer measurements. *Geophys. Res. Lett.*, *116*(A7), A07226. https://doi.org/10.1029/2010JA016226

Vampola, A. L., and Korth A. (1992). Eletron drift echoes in the inner magnetosphere. *Geophys. Res. Lett.*, *19*, 625-628. https://doi.org/10.1029/92GL00121

Wilken, B., Goertz, C. K., Baker, D. N., Higbie, P. R., and Fritz, T. A. (1982). The SSC on July 29, 1977 and its propagation within the magnetosphere. *J. Geophys. Res.*, *87*(A8), 5901-5910. https://doi.org/10.1029/JA087iA08p05901

Wilken, B., Baker, D. N., Higbie, P. R., Fritz, T. A., Olson, W. P., and Pfitzer, K. A. (1986). Magnetospheric configuration and energetic particle effects associated with a SSC: A case study of the CDAW 6 event on March 22, 1979. *J. Geophys. Res.*, *91*(A2), 1459-1473. https://doi.org/10.1029/JA091iA02p01459

Wilken, B., Daly, P. W., Mall， U., Aarsnes, K., Baker, D. N., Belian, R. D., Blake, J. B., Borg, H., Büchner, J., Carter, M., Fennell, J. F., Friedel, R., Fritz, T. A., Gliem, F., Grande, M., Kecskemety, K., Kettmann, G., Korth, A., Livi, S., McKenna-Lawlor1, S., Mursula1, K., Nikutowski, B., Perry, C. H., Pu1, Z. Y., Roeder, J., Reeves, G. D., Sarris, E. T., Sandahl1, I., Søraas, Woch, F., J., and Zong, Q.-G. (2001). First results from the rapid imaging energetic particle spectrometer on board cluster. *Ann. Geophys.*, *19*, 1355-1366. https://doi.org/10.5194/angeo-19-1355-2001

Wright, D. M., Yeoman, T. K., Rae, I. J., Storey, J., Stockton-Chalk, A. B., Roeder, J. L., and Trattner, K. J. (2001). Ground-based and Polar spacecraft observations of a giant (Pg) pulsation and its associated source mechanism. *J. Geophys. Res.*, *106*(A6), 10837-10852. https://doi.org/10.1029/2001JA900022

Wygant, J., Mozer, F., Temerin, M., Blake, J., Maynard, N., Singer, H., and Smiddy, M. (1994). Large amplitude electric and magnetic field signatures in the inner magnetosphere during injection of 15 MeV electron drift echoes. *Geophys. Res. Lett.*,, *21*, 1739-1742. https://doi.org/10.1029/94GL00375

Yang, B., Zong, Q.-G., Wang, Y. F., Fu, S. Y., Song, P., Fu, H. S., Korth, A., Tian, T., and Reme, H. (2010). Cluster observations of simultaneous resonant interactions of ULF waves with energetic electrons and thermal ion species in the inner magnetosphere. *J. Geophys. Res.*, *115*(A2), A02214. https://doi.org/10.1029/2009JA014542

Yang, B., Q.-G. Zong, S. Y. Fu, X. Li, A. Korth, H. S. Fu, C. Yue, and H. Reme (2011a). The role of ULF waves interacting with oxygen ions at the outer ring current during storm times. *J. Geophys. Res.*, *116*(A1), A01203. https://doi.org/10.1029/2010JA015683

Yang, B., Q.-G. Zong, S. Y. Fu, K. Takahashi, X. Li, Y. F. Wang, Z. Y. Pu, H. S. Fu, H. Reme, C. Yue, H. Zheng, and C. Sheng (2011b). Pitch angle evolutions of oxygen ions driven by storm time ULF poloidal standing waves. *J. Geophys. Res.*, *116*(A3), A03207. https://doi.org/10.1029/2010JA016047

Yue, C., W. Li, Y. Nishimura, Q. G. Zong, Q. L. Ma, J. Bortnik, R.M. Thorne, G. D. Reeves, H. E. Spence, C. A. Kletzing, J. R. Wygant, and M. J. Nicolls (2016). Rapid enhancement of low-energy (<100 eV) ion flux in response to interplanetary shocks based on two Van Allen probes case studies: Implications for source regions and heating mechanisms. *J. Geophys. Res.*, *121*, 6430-6443. https://doi.org/10.1002/2016JA022808

Zhang, X. Y., Zong, Q. G., Yang, B., and Wang, Y. F. (2009). Numerical simulation of magnetospheric ULF waves excited by positive and negative impulses of solar wind dynamic pressure. *Sci. China Ser. E-Tech. Sci.*, *52*, 2286-2894. https://doi.org/10.1007/s11431-009-0270-6

Zhang, X. Y., Zong, Q.-G., Wang, Y. F., Zhang, H., Xie, L., Fu, S. Y., Yuan, C. J., Yue, C., Yang, B., and Pu, Z. Y. (2010). ULF waves excited by negative/positive solar wind dynamic pressure impulses at geosynchronous orbit. *J. Geophys. Res.*, *115*(A10), A10221. https://doi.org/10.1029/2009JA015016

Zong, Q-G., Wilken, B., Fu, S.-Y., Fritz, T. A., Korth, A., Hasebe, N., Williams, D. J., and Pu, Z.-Y. (2001). Ring current oxygen ions escaping into the magnetosheath. *J. Geophys. Res.*, *106*(A11), 25541-25556. https://doi.org/10.1029/2000JA000127

Zong, Q-G., Zhou, X.-Z., Li, X., Song, P., Fu, S. Y., Baker, D. N., Pu, Z. Y., Fritz, T. A., Daly, P., Balogh, A., and Réme, H. (2007). Ultralow frequency modulation of energetic particles in the dayside magnetosphere. *Geophys. Res. Lett.*, *34*, L12105. https://doi.org/10.1029/2007GL029915

Zong, Q-G., Wang, Y. F., Yang, B., Fu, S. Y., Pu, Z. Y., Xie, L., and Fritz, T. A. (2008). Recent progress on ULF wave and its interactions with energetic particles in the inner magnetosphere. *Sci. China Ser. E*: *Tech. Sci.*, *51*, 1620-1625. https://doi.org/10.1007/s11431-008-0253-z

Zong, Q-G., Zhou, X.-Z., Wang, Y. F., Li, X., Song, P., Baker, D. N., Fritz, T. A., Daly, P. W., Dunlop, M., and Pedersen, A. (2009). Energetic electron response to ULF waves induced by interplanetary shocks in the outer radiation belt. *J. Geophys. Res.*, *114*(A10), A10204. https://doi.org/10.1029/2009JA014393

Zong, Q-G., Wang, Y. F., Yuan, C. J., Yang, B., Wang, C. R., and Zhang, X. Y. (2011). Fast acceleration of "killer" electrons and energetic ions by interplanetary shock stimulated ULF waves in the inner magnetosphere. *Chin. Sci. Bull.*, *56*, 1188-1201. https://doi.org/10.1007/s11434-010-4308-8

Zong, Q-G., Wang, Y. F., Zhang, H., Fu, S. Y., Zhang, H., Wang, C. R., Yuan, C. J., and Vogiatzis, I. (2012). Fast acceleration of inner magnetospheric hydrogen and oxygen ions by shock induced ULF waves. *J. Geophys. Res.*, *117*(A11), A11206. https://doi.org/10.1029/2012JA018024